WAVELET BASED DECOMPOSITION OF NATURAL IMAGES IN INDEPENDENT RESOLUTION LEVELS

Antonio Turiel

Laboratoire de Physique Statistique
Ecole Normale Supérieure
24, rue Lhomond
75231 Paris Cedex 05, France
Antonio.Turiel@lps.ens.fr

Néstor Parga

Departamento de Física Teórica
Universidad Autónoma de Madrid
Ciudad Universitaria de Cantoblanco
28049 Madrid, Spain
parga@delta.ft.uam.es

ABSTRACT

Efficient coding of natural scenes requires the use of a proper filter to reduce their redundancy. In this work we show that nongaussian statistical properties of natural scenes uniquely define a wavelet filter that decomposes the image in a set of statistically independent resolution levels. The spatial statistical dependences still present at a fixed scale are extremely short-ranged.

1. INTRODUCTION

Given the complexity and degree of redundancy of natural images, the early visual system had to find good coding procedures to represent the visual stimuli internally. To achieve this goal, the visual system must have learnt the regularities present in the environment where the organism lived [1]. If there are image features that tend to appear together, a cell responding quasi-optimally to them is rather likely to exist. To find such a representation one has first to understand the statistical properties of visual scenes common in the environment. In particular, the relevance of the second order statistics has been pointed out some time ago [2], and internal representations that eliminate these correlations have been discussed [3]. However, even if whitening represents an improvement of the code, it still leaves much geometrical structure that should be dealt with more properly [4]. A more systematic study of statistical regularities that go beyond the two-point correlations has began rather recently [5, 6, 7]. A novel approach to understand the statistical properties of natural images has been proposed in [6] where the nongaussian statistics of changes in contrast has been characterized and explained by means of a stochastic multiplicative process: Contrast changes at a given scale are obtained from those at a coarser scale by multiplication with an independent random variable. A very rich geometrical structure has emerged from those studies: contrast changes are organized in such a way that pixels in the image can be classified according to the strength of the singularities of the contrast gradient [7]. It was also checked that the multiplicative process is present in very different sets of images and in color natural images [8].

We present in this work a procedure to split any image in a collection of successive, independent resolution levels. This decomposition is based on the multiplicative process and on projecting the image over a intrinsic wavelet which is defined statistically by the requirement of independence between the resolution layers.

2. WAVELET PROJECTIONS AND MULTISCALING

Natural images will be described by means their luminosity contrast $c(\vec{x})$, which is defined as $c(\vec{x}) =$

This work was funded by a Spanish grant PB96-0047. A. Turiel is financially supported by a fellowship from the Spanish Ministry of Education.

$I(\vec{x}) - \langle I \rangle$, where $I(\vec{x})$ is the field of luminosities and $\langle I \rangle$ its average value across the image ensemble. [1] This quantity lacks a definite scale, what is seen in the power law characterization of its power spectrum [9] and in a multiscaling set of variables, each exhibiting power law behaviour [6, 7]. These properties can be used advantegeously to design coding strategies which reduce the redundancy; this has been already done using the power spectrum characterization (see e.g. [10]). As it will be shown in this work, there exists a wavelet representation adapted to the multiscaling power laws found in [6] that produces a more efficient coding.

In order to focus the contrast at a given resolution level it will be projected onto convenient traslations and dilations of a wavelet $\tilde{\Psi}(\vec{x})$ [11]. The shift to the point $\vec{x}_0$ and the dilation of scale factor r of this wavelet will be denoted as $\tilde{\Psi}_r(\vec{x} - \vec{x}_0) \equiv \tilde{\Psi}(\frac{\vec{x}-\vec{x}_0}{r})$. The **wavelet projections** $T^r_{\tilde{\Psi}} c(\vec{x}_0)$ of the field of luminosity contrast,

$$T^r_{\tilde{\Psi}} c(\vec{x}_0) \;=\; r^{-2} \int d\vec{x}\; \tilde{\Psi}_r(\vec{x} - \vec{x}_0) c(\vec{x}) \qquad (1)$$

characterize completely the image. This is the reason of the name "multiresolution analysis": the wavelet projection is a description of $c(\vec{x})$ at the point $\vec{x}_0$ when the image is observed at a variable scale r. For notational convenience the wavelet projections $T^r_{\tilde{\Psi}} c(\vec{x}_0)$ will be denoted as $\alpha_r(\vec{x}_0)$.

The question now arises of how the distribution of $\alpha_l(\vec{x})$ could be related to the distribution of $\alpha_L(\vec{x})$, for two different scales $l < L$. This was discussed in [6, 7] for the marginal distribution of $\alpha_l(\vec{x})$ (since the marginal distribution disregards the space index $\vec{x}$ this stochastic variable will be denoted as α_l). The answer is simple: they are related by a multiplicative process. Denoting by η_{lL} the multiplicative stochastic variable, this means that

$$\alpha_l \;=\; \eta_{lL}\, \alpha_L \;\;, \qquad (2)$$

where the random variable η_{lL} is independent of α_L. This scale transformation can be thought of as composed of smaller changes; in fact the multiplicative character of the process implies that it should be possible to go from scale L to l through an intermediate scale r; this gives the factors η_{rL} and η_{lr} which are related to the global transformation by $\eta_{lL} = \eta_{lr}\eta_{rL}$.

The process for arbitrary changes in scale was discussed in [6, 7] where it was shown that the random variable η_{lL} follows a log-Poisson distribution. [2] This process can be justified as follows. As the scale is gradually reduced from L to l the wavelet $\tilde{\Psi}_r$ becomes more concentrated around the point $\vec{x}_0$, in this way it explores its neighborhood with finer detail and, at the same time, gives less weight to the contrast at pixels that now appear closer to its tail. Depending on the type of singularitites of the contrast, it may happen that under a small scale transformation δ_r its wavelet projection undergoes (with some probability) a discontinuous change. [3] We will refer to this effect by saying that a modulation has occurred. The simplest way to model this situation is to assume that each time that a modulation occurs the wavelet projection $\alpha_{r-\delta_r}$ acquires a factor β $(0 \leq \beta < 1)$ relative to α_r. Apart from this, since both the contrast and the wavelet can take positive and negative values, the sign of $\alpha_{r-\delta_r}$ will also change with respect to that of α_r.

To complete the description of the statistics of the α's it will be assumed that:

- modulations are independent events. The average number of them contained in the change of scale $(\ln L - \ln l)$ is denoted by s,
- the sign of the η's is a random variable independent of its absolute value. Besides, plus and minus signs are equally probable,
- the image ensemble is translational invariant,

[1] From now on the angular brackets $\langle \ldots \rangle$ will denote the average over an ensemble of images.

[2] This kind of multiplicative process appears in a wide variety of systems, for instance in turbulent flows (see [12] and references therein)

[3] The singularity could be hidden by a regular piece of the contrast. If this is the case the singular behaviour will show up if the wavelet is chosen such that it makes the regular part to vanish. See [7] for a full discussion of this point.

- the multiplicative process is scale invariant.

These hypotheses uniquely define the distribution $\rho_{|\eta_{lL}|}$ of the multiplicative process. Under a finite change from L to l, there will be n modulations with probability p_n that, given the first assumption, is Poisson:

$$p_n = \frac{s^n}{n!} e^{-s} \tag{3}$$

The value of $|\eta_{lL}|$ after n modulations is proportional to β^n: $|\eta_{lL}| = \beta^n M(l,L)$. The fact that the proportionality constant is not one can be understood by noticing that if no modulations occur (i.e., $n = 0$), α_l keeps as much singular structure at the scale l as that seen at the coarser scale L.

The dependence of $M(l,L)$ on the scales l and L can be obtained by invoking the scale invariance property of the multiplicative process. In this case, it can only depend on the ratio l/L, that is $M(l,L) = M(\frac{l}{L})$. A standard argument shows that it has to be a power law: if the change from L to l is done through an intermediate scale r, then because of the multiplicative character of the process we have $M(\frac{l}{L}) = M(\frac{l}{r})M(\frac{r}{L})$, which can only be satisfied if $M(\frac{l}{L}) = \left(\frac{l}{L}\right)^{-\Delta_c}$. The exponent Δ_c is another parameter of the model. Taking all these arguments into account, the distribution $\rho_{|\eta_{lL}|}(\ln|\eta_{lL}|)$ can be expressed as:

$$\rho_{|\eta_{lL}|} = e^{-s} \sum_{n=0}^{\infty} \frac{s^n}{n!} \delta\left(\ln|\eta_{lL}| - n\ln\beta - \Delta_c \ln\frac{L}{l}\right). \tag{4}$$

Up to now we have considered s, β and Δ_c as independent parameters. However translational invariance fixes one of them. In fact, from the definition of the α's, eq. (1), one checks that its average over a translational invariant ensemble of images is proportional to the scale [7]. In turn, taking the average on both sides of eq. (2), this implies that

$$\langle|\eta_{lL}|\rangle = \frac{l}{L} \ . \tag{5}$$

Imposing this condition over the value of this average obtained from the distribution in eq. (4) one has:

$$s = \frac{\Delta_c - 1}{1-\beta} \ln\frac{L}{r} \ , \tag{6}$$

from where the average number of modulations per unit of change in scale is $\bar{s} = \frac{\Delta_c - 1}{1-\beta}$.

The existence of a multiplicative process has direct consequences on the scaling properties of the moments of α_r. Let us denote these moments by $\langle\alpha_r^p\rangle$. If the log-Poisson model holds, then from eq. (4) it is easy to check that the moments have a property called Self-Similarity (SS),

$$\langle\alpha_r^p\rangle = A_p \, r^{p+\tau_p} \ , \tag{7}$$

where the τ_p's are the SS exponents. Notice that this also implies that any moment can be expressed as a power of the moment of order q. Choosing $q = 2$ this means that

$$r^{-p}\langle\alpha_r^p\rangle = A(p,2)\left[r^{-2}\langle\alpha_r^2\rangle\right]^{\rho(p,2)} \ , \tag{8}$$

This relation could hold even when SS is not true. It is called Extended Self-Similarity (ESS) [13]. The $\rho(p,2)$'s are the ESS exponents and the $A(p,2)$'s are geometrical factors. The exponents $\rho(p,2)$ can be predicted using the distribution of the multiplicative process, eq. (4), to evaluate the moments of order p in eq. (2). This computation yields

$$\rho(p,2) = \frac{p}{1-\beta} - \frac{1-\beta^p}{(1-\beta)^2} \ . \tag{9}$$

Let us notice that although the model has two parameters, β and $\bar{s}$, the ESS exponents $\rho(p,2)$ depend only on the modulation parameter β. There is a simple relation between τ_p and $\rho(p,2)$:

$$\tau_p = -\bar{s}(1-\beta)^2 \, \rho(p,2) \ , \tag{10}$$

Conversely, it can be proven that if SS and ESS hold and the exponents $\rho(p,2)$ verify eq. (9), then α_r can be described in terms of a multiplicative process (eq. (2)) of the log-Poisson type (eq. (4)). It is then enough to check eq. (9), from where the existence of a log-Poisson process is derived.

All these properties (SS,ESS and log-Poisson process) have been experimentally found to hold for certain class of wavelets (such that some of their low order moments are zero), and for a wide

variety of collections of natural images, from forest pictures ([6, 7]) to open lands, city scenes and even for the chromatic components in color images [8].

2.1. Wavelet basis and multiresolution analysis

Let us now consider the projection of the contrast $c(\vec{x})$ on a dyadic wavelet set $\tilde{\Psi}_{j\vec{k}}(\vec{x}) = \tilde{\Psi}(2^j\vec{x} - \vec{k})$. The wavelet $\Psi_{j\vec{k}}$ corresponds to a scale factor $r = 2^{-j}$, $j \in \mathcal{Z}$ and displacement point $\vec{x}_0 = 2^{-j}\vec{k}$. Here $\vec{k} \equiv (k_1, k_2)$, with $k_1, k_2 \in \mathcal{Z}$[11]. If the discrete basis is complete, then the contrast can be expanded in a wavelet basis orthogonal to $\tilde{\Psi}$ using the wavelet projections as coefficients. The dual basis $\Psi_{j\vec{k}}$ verifies that:

$$\langle \tilde{\Psi}_{j\vec{k}} | \Psi_{j'\vec{k}'} \rangle \;=\; 2^{-2j}\delta_{jj'}\delta_{\vec{k}\vec{k}'} \tag{11}$$

and the contrast $c(\vec{x})$ can then be expressed as:

$$c(\vec{x}) \;=\; \sum_{j,\vec{k}} \alpha_{j\vec{k}}\, \Psi_{j\vec{k}}(\vec{x}) \tag{12}$$

where $\alpha_{j\vec{k}} = T_{\tilde{\Psi}}^{2^{-j}} c(2^{-j}\vec{k})$. The wavelet basis generated by Ψ will be called the **representation basis**. Its dual basis, defined by $\tilde{\Psi}$ will be referred to as the **analizer basis**. Once one of these basis is known, the other is completely defined by eq. (11).

The discussion in the previous section refers to the properties of the marginal distribution of the wavelet coefficients. The analysis to the variables $\alpha_{j\vec{k}}$ themselves; for them the multiplicative process eq. (2) is generalized to:

$$\alpha_{j\vec{k}} \;=\; \eta_{j\vec{k}}\, \alpha_{j-1,\left[\frac{\vec{k}}{2}\right]} \tag{13}$$

where $[\vec{\kappa}]$ denotes the vector with components given by the integer part (rouding down) of those of $\vec{\kappa}$. We will require the variables $\eta_{j\vec{k}}$ to be statistically independent of $\alpha_{j-1,\left[\frac{\vec{k}}{2}\right]}$. Besides, according to the multiplicative process for the marginals, eq. (2), the distributions of all the $\eta_{j\vec{k}}$ should be identical, because they only depend on the ratio of scales, which is always 2 for $\alpha_{j\vec{k}}$, $\alpha_{j-1,\left[\frac{\vec{k}}{2}\right]}$. The $\eta_{j\vec{k}}$ will be given rise to the independent resolution levels of the image.

We will show in the next section that natural images possess an intrinsic wavelet for which eq. (13) is fulfilled *point by point*. This means that the equality holds for any image, at any scale and position and that the variables $\eta_{j\vec{k}}$ can be extracted directly from[4] :

$$\eta_{j\vec{k}} \;=\; \frac{\alpha_{j\vec{k}}}{\alpha_{j-1,\left[\frac{\vec{k}}{2}\right]}} \tag{14}$$

The representation wavelet Ψ (and so the analizer $\tilde{\Psi}$ is uniquely defined once the assumptions that the η's obtained from eq. (14) are scale independent and equally distributed variables are stated, and then the representation wavelet Ψ can be experimentally obtained from a statistical analysis of the image ensemble. The validity of these two hypothesis on the η's has to be verified *a posteriori*, once the wavelet is known. This is done in Section 4 as follows: first the the analizer wavelet $\tilde{\Psi}$ is obtained from the representation wavelet Ψ. In turn, $\tilde{\Psi}$ can be used to evaluate the coefficients $\alpha_{j\vec{k}}$'s and from them the $\eta_{j\vec{k}}$'s. Once these are known it is finally checked that they are indeed scale-independent, identically distributed random variables, so checking the self-consistency of the multiplicative process model.

3. THE MOTHER WAVELET

We suppose that the contrast field obtained from our image dataset can be expanded as a superposition of wavelets, eq. (12), and that the $\alpha_{j\vec{k}}$'s verify eq. (13), where the $\eta_{j\vec{k}}$'s are scale independent equally distributed variables. Since the images have finite size we will take $j \geq 0$ where $\Psi_{0\vec{0}}$ covers the whole image and it represents the mother wavelet, $\Psi_{0\vec{0}} \equiv \Psi$. For the same reason,

[4] The random, independent variable $\log \eta_{j\vec{k}}$ could then be expressed as a linear relation between the logarithms of the variables at the two scales. This property has also been discussed in [14], although the existence of a multiplicative process was not noticed. Let us also observe that this property just holds for the wavelet projections over the correct wavelet $\tilde{\Psi}$ which is derived in the present work.

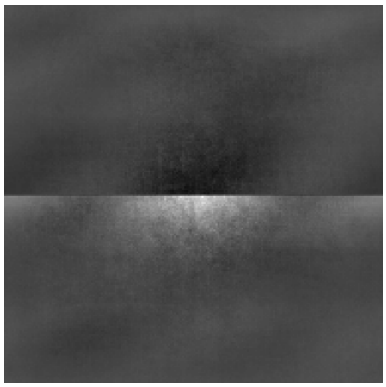

Figure 1: Representation wavelet Ψ for the image ensemble. The function is represented in gray levels, the darkest points indicate the sites where it takes its smallest values.

the range of $\vec{k} = (k_1, k_2)$ at the scale j is bounded as: $k_1, k_2 = 0, 1, ..., 2^j - 1$.

Averaging $c(\vec{x})$ at each point $\vec{x}$, it is found that the average contrast can be represented as a simple wavelet superposition: $\mathcal{C}(\vec{x}) \equiv \langle c \rangle(\vec{x}) \propto \alpha_{0\vec{0}} \sum_{j,\vec{k}} \overline{|\eta|}^j \Psi_{j\vec{k}}(\vec{x})$. Here $\overline{|\eta|}$ is the first order moment of the distribution of the $|\eta|$'s, and we have used the assumptions that all the $\eta_{j\vec{k}}$'s have the same marginal distribution and are independent across the scales. By Fourier transforming this field, $\hat{\mathcal{C}}(\vec{f})$, one easily obtains the Fourier transform of the representation wavelet, $\hat{\Psi}(\vec{f})$, that reads:

$$\hat{\Psi}(\vec{f}) \;=\; \frac{1}{\alpha_{0\vec{0}}} \left[\hat{\mathcal{C}}(\vec{f}) - \frac{\overline{|\eta|}}{4} \frac{\Lambda(\vec{f})}{\Lambda(\frac{\vec{f}}{2})} \hat{\mathcal{C}}(\frac{\vec{f}}{2}) \right] \qquad (15)$$

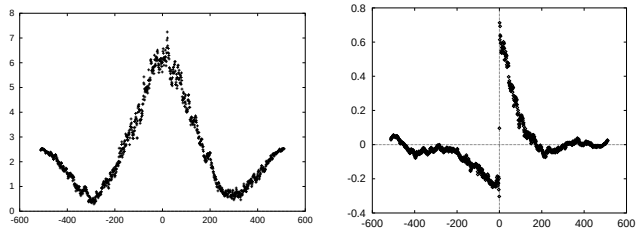

Figure 2: The wavelet Ψ along the horizontal (left) and the vertical axis (right).

where $\Lambda(\vec{f}) = (1 - e^{-2\pi i f_1})(1 - e^{-2\pi i f_2})$. This expression is very appealing. The right hand side compares the average contrast at two consecutive scales (related by a factor 2), and it expresses that the wavelet is obtained as an observation of the scale transformation properties of the images. The average $\overline{|\eta|}$ has an *a priori* known value: $\overline{|\eta|} = \frac{1}{2}$ (see eq. (5)). This allows to use eq. (15) with no *a priori* knowledge about the data.

To obtain experimentally the representation wavelet, eq. (15) was applied to a large ensemble of natural images. The data were 200 1024×1024 images selected at random from van Hateren's dataset [15]. Figure 1 shows the representation wavelet obtained with this procedure. It exhibits two clear features: it is right-left symmetric and roughly up-down antisymmetric with a sharp central discontinuity (see Figure 2). The first property is expected: our world remains statistically unchanged when it is reflected from left to right. The rough up-down antisymmetry and the related discontinuity are probably due to the sharp contrast between the sky and the ground.

4. THE PROJECTION INTO THE EXPERIMENTAL BASIS

Once the analizer wavelet is obtained, it can be used to evaluate the coefficients $\alpha_{j\vec{k}}$ and from them, using eq. (14), the coefficients $\eta_{j\vec{k}}$. Then, it is possible to check whether the $\eta_{j\vec{k}}$ are scale-independent, identically distributed variables. In the affirmative case, this fact self-consistently demonstrates that eq. (15) is the intrinsic wavelet we are looking for. It is immediate to check that the signs of the η's are independent of their absolute values, $|\eta|$, and also scale-independent, so it is only necessary to verify the independence of the $|\eta|$'s.

The mutual dependence among the $|\eta_{j\vec{k}}|$'s was estimated by computing the mutual informations between two $|\eta|$'s. As the number of possible pairs is very large, only two types of mutual informations were considered, which should be maximal by construction: those between consecutive scales ($j-1$ and j) at equivalent positions, and those between consecutive spatial positions ($\vec{k}$ and $\vec{k} + \vec{d}$, where the components of $\vec{d}$ take only the values 0

and 1) at a fixed scale j.

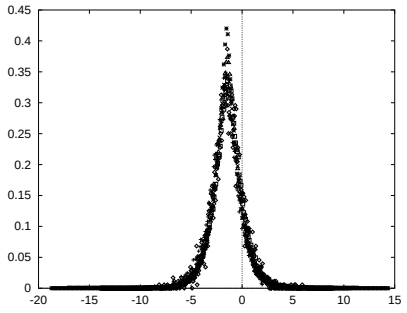

Figure 3: P.d.f.'s of $\ln|\eta_j|$ at the scales $j = 2$ (diamonds), 3 (crosses), 4 (squares), 5 (x), 6 (triangles) and 7 (crossed x).

Both quantities, denoted as μ_j and $\mu_{j\vec{d}}$ respectively, are always positive and give a measure of statistical dependence: they represent the number of bits of information shared by the variables. Two variables will be independent if and only if they share 0 bits. The observed values of μ_j are very close to 0 ($|\mu_j| < 10^{-4}$ bits, $j > 3$), what confirms rather well the independence of the $\eta_{j\vec{k}}$'s under changes of scale. On the contrary, the mutual informations $\mu_{j\vec{d}}$ are by no means negligible, although they are extremely short-ranged: the variables $\eta_{j\vec{k}}$ and $\eta_{j\vec{k}'}$ are statistically dependent when they are one pixel apart ($\mu_{j\vec{d}} \approx 0.13$ bits); after that distance the mutual information $\mu_{j\vec{d}}$ decays dramatically. It is important to remark that there is no need of spatial independence of the $\eta_{j\vec{k}}$'s in our wavelet model. For this reason, although short-ranged, the observed dependence is a significant source of information about the remaining statistical structure at a fixed resolution layer. On the other hand, the η's define a system of almost completely independent variables.

To confirm the validity of the wavelet representation, eqs. (12) and (15), one has still to check that the η's are identically distributed. Figure 3 exhibits the distribution of $\ln|\eta_j|$ for different scales j. The correspondence between them is really very good.

5. WAVELET TRANSPARENCY AND DECORRELATION

It has been frequently argued that the the signal that arrives to the primary visual cortex has been already decorrelated in previous stages of the visual system [3, 16]. In this case, V1 would take care of coding more complex aspects of images. In this regard, the way in which the mother wavelet is constructed guarantees a remarkable property of transparency to the power spectrum: it defines a code that is somewhat independent of the second order statistics of the images. The power spectrum of natural images exhibits a power law behaviour, $S(\vec{f}) \sim f^{-(2-\epsilon)}$ [2]. Under the assumption of translational invariance, the application of the decorrelating filter to the contrast is equivalent to multiplication in the Fourier domain by $f^{1-\frac{\epsilon}{2}}$. Denoting the decorrelated contrast as $\mathbf{D}c(\vec{x})$, it is immediate to see that it has a representation similar to eq. (12):

$$\mathbf{D}c(\vec{x}) \;=\; \sum_{j\vec{k}} \alpha'_{j\vec{k}}\, \mathbf{D}\Psi_{j\vec{k}}(\vec{x}) \quad , \qquad (16)$$

where $\mathbf{D}\Psi$ indicates the application of the decorrelating operator to the representation wavelet and $\alpha'_{j\vec{k}} = 2^{j(1-\frac{\epsilon}{2})}\alpha_{j\vec{k}}$. Defining now $\eta'_{j\vec{k}} = 2^{1-\frac{\epsilon}{2}}\eta_{j\vec{k}}$ it is concluded that the decorrelated images also posses a random multiplicative process. The new representation wavelet $\mathbf{D}\Psi$ can be obtained from an ensemble of decorrelated images by means of eq. (15). It is known that the value of the exponent ϵ has fluctuations from image to image [9]. The relevance of the wavelet transparency is that if the visual stimulus has been decorrelated before it reaches V1, this area can use the type of filters described in this paper regardless of the precise exponent of the power spectrum.

6. CONCLUSIONS

We have shown that images can be represented as multiresolution objects in terms of an appropriate wavelet basis Ψ, in which each resolution level is an independent image. One of the advantages of this representation is that it is based on the observed properties of the contrast gradient [6, 7],

what in turn leads to an automatic reduction of the redundancy. At the same time the spatial correlations at a given scale are short-ranged, but still informative.

These results have been obtained with the simplest wavelet expansion, but the tools presented in this work can be taken as the starting point to look for more realistic visual filters. This search should be directed by the experimental observation that cells in V1 are edge detectors. From this perspective, the expansion in eq. (12) should be generalized to include an orientational degree of freedom. Filters of this type have been proposed in [17] and found from an independent component analysis of natural images [18] . These studies should be combined with the use of overcomplete basis, this introduces redundancy but the representation becomes stable under small changes in the images [19]

7. REFERENCES

[1] Barlow H. B., in *Sensory Communication* (ed. Rosenblith W.) pp. 217. (M.I.T. Press, Cambridge MA, 1961)

[2] Field D. J., *J. Opt. Soc. Am.* **4**: 2379-2394 (1987)

[3] Atick J. J. *Network* **3**: 213-251 (1992); van Hateren J.H. *J. Comp. Physiology A* **171**: 157-170 (1992)

[4] Field D. J., in *Wavelets, Fractals, and Fourier Transforms*. Eds. Farge M., Hunt J.C.R. & Vassilicos J.C., pp. 151-193. Clarendon Press, Oxford (1993).

[5] Ruderman D. & Bialek W., *Phys. Rev. Lett.* **73**: 814 (1994); Ruderman D., *Network* **5**: 517-548 (1994)

[6] Turiel A., Mato G., Parga N. & Nadal J.-P. *Phys. Rev. Lett.* **80**: 1098-1101 (1998); Turiel A., Mato G., Parga N. & Nadal J.-P. *Proc. of NIPS'97*. MIT Press, Cambridge, MA (1998).

[7] Turiel A. & Parga N. *Neural Computation* **12**: 853-883 (2000)

[8] Nevado A., Parga N & Turiel A. Sub. to *Network* (1999); Turiel A., Parga N., Ruderman D. & Cronin T.W., Sub. to *Phys. Rev. E* (1999); Turiel A. & del Pozo A. Sub. to *Phys. Rev. E* (1999)

[9] Tollhurst D. J., Tadmor Y. & Tang Chao, *Ophthal. Physiol. Opt.* **12**: 229-232 (1992)

[10] Atick J. J.*Network* **3** 213-251, 1992.

[11] Daubechies I. *"Ten Lectures on Wavelets"*. CBMS-NSF Series in Ap. Math. *Capital City Press*. Montpelier, Vermont (1992)

[12] Frisch U., *Turbulence*, Cambridge Univ. Press (1995)

[13] Benzi R., Ciliberto S., Baudet C., Ruiz Chavarria G. and Tripiccione C., *Europhys. Lett.* **24** 275-279 (1993)

[14] Buccigrossi R.W. and Simoncelli E.P., *IEEE Trans Image Processing* **8**, 1688-1701, (1999).

[15] Hateren, J.H. van & Schaaf, A. van der *Proc.R.Soc.Lond. B* **265**: 359-366 (1998)

[16] Yang Dan, Atick J. & Clay Reid R., *J. of Neuroscience* **16**: 3351-3362 (1996)

[17] Daugman J.G., , *IEEE Transactions on Biomedical Engineering* **36**: 107-114 (1989)

[18] Bell A.J. & Sejnowski T.J., *Vision Research* **37**: 3327-3338 (1997)

[19] Simoncelli E.P., Freeman W.T., Adelson E.H. & Heeger D.J., *IEEE Transactions on Information Theory* **382**: 587-607 (1992); Olshausen B.A. & Field D.J., *Vision Research* **37**: 3311-3325 (1997)